

## Adsorption and Separation of Reactive Aromatic Isomers and Generation and Stabilization of Their Radicals within Cadmium(II)–Triazole Metal–Organic Confined Space in a Single-Crystal-to-Single-Crystal Fashion

Qi-Kui Liu, Jian-Ping Ma, and Yu-Bin Dong\*

College of Chemistry, Chemical Engineering and Materials Science, Key Laboratory of Molecular and Nano Probes, Engineering Research Center of Pesticide and Medicine Intermediate Clean Production, Ministry of Education, Shandong Normal University, Jinan 250014, People's Republic of China

Received March 3, 2010; E-mail: yubindong@sdu.edu.cn

**Abstract:** A series of reactive group functionalized aromatics, namely 2-furaldehyde, 3-furaldehyde, 2-thenaldehyde, 3-thenaldehyde, *o*-toluidine, *m*-toluidine, *p*-toluidine, and aniline, can be absorbed by a CdL<sub>2</sub> (**1**; L = 4-amino-3,5-bis(4-pyridyl-3-phenyl)-1,2,4-triazole) porous framework in both vapor and liquid phases to generate new G<sub>n</sub>CdL<sub>2</sub> (*n* = 1, 2) host–guest complexes. In addition, the CdL<sub>2</sub> framework can be a shield to protect the active functional group (–CHO and –NH<sub>2</sub>) substituted guests from reaction with the outside medium containing their reaction partners. That is, aldehyde-substituted guests within the CdL<sub>2</sub> host become “stable” in the aniline phase and vice versa. Moreover, **1** displays a very strict selectivity for these reactive group substituted aromatic isomers and can completely separate these guest isomers under mild conditions (i.e., 2-furaldehyde vs 3-furaldehyde, 2-thenaldehyde vs 3-thenaldehyde, and *o*-toluidine vs *m*-toluidine vs *p*-toluidine). All adsorptions and separations are directly performed on the single crystals of **1**. More interestingly, these reactive group substituted aromatics readily transform to the corresponding radicals within the CdL<sub>2</sub> host upon ambient light or UV light (355 nm) irradiation. Furthermore, the generated organic radicals are alive for 1 month within the interior cavity in air under ambient conditions. Simple organic radicals are highly reactive short-lived species, and they cannot be generally isolated and conserved under ambient conditions. Thus, the CdL<sub>2</sub> host herein could be considered as a radical generator and storage vessel.

### Introduction

One of the most promising applications for metal–organic frameworks (MOFs)<sup>1</sup> might be their use as porous materials for storage, separation, and purification. The recent upsurge in MOFs reflects their application in the storage and separation of gases such as hydrogen, methane, and carbon dioxide.<sup>2</sup> In contrast, the adsorption and separation of larger organic compounds is a very rarely explored field, although a handful of MOFs that are able to selectively adsorb and separate inert aromatic hydrocarbons have been reported very recently.<sup>3</sup> To date, to our knowledge, the adsorption and separation of the aromatic isomers with reactive functional groups are unprec-

edented. Reactive groups attached to aromatic rings, such as –CHO and –NH<sub>2</sub> groups, might react with the host framework (including organic components and metal ions) to introduce a new functionality. Thus, the adsorption and separation of reactive organic aromatics based on MOFs are limited. Such chemistry, now termed as “postsynthetic covalent modification”,<sup>4</sup> is used as an attractive alternative approach to prepare the MOFs with new functionalized pores. “Postsynthetic covalent modification”, on the other hand, reflects the inherent

- (1) (a) Moulton, B.; Zaworotko, M. J. *Chem. Rev.* **2001**, *101*, 1629. (b) Yaghi, O. M.; O’Keeffe, M.; Ockwig, N. W.; Chae, H. K.; Eddaoudi, M.; Kim, J. *Nature* **2003**, *423*, 706. (c) Kitagawa, S.; Kitaura, R.; Noro, S.-I. *Angew. Chem., Int. Ed.* **2004**, *43*, 2334. (d) Kubas, G. *Chem. Rev.* **2007**, *107*, 4152.
- (2) (a) Eddaoudi, M.; Kim, J.; Rosi, N.; Vodak, D.; Wachter, J.; O’Keeffe, M.; Yaghi, O. *Science* **2002**, *295*, 469. (b) Bourrelly, S.; Llewellyn, P.; Serre, C.; Millange, F.; Loiseau, T.; Férey, G. *J. Am. Chem. Soc.* **2005**, *127*, 13519. (c) Panella, B.; Hirscher, M.; Puetter, H.; Mueller, U. *Adv. Funct. Mater.* **2006**, *16*, 520. (d) Liu, Y.; Eubank, J. F.; Cairns, A. J.; Eckert, J.; Kravtsov, V. C.; Luebke, R.; Eddaoudi, M. *Angew. Chem., Int. Ed.* **2007**, *46*, 3278. (e) Phan, A.; Doonan, C. J.; Uribe-Romo, F. J.; Knobler, C. B.; O’Keeffe, M.; Yaghi, O. M. *Acc. Chem. Res.* **2010**, *43*, 58.

- (3) (a) Deng, H.; Doonan, C. J.; Furukawa, H.; Ferreira, R. B.; Towne, J.; Knobler, C. B.; Wang, B.; Yaghi, O. M. *Science* **2010**, *327*, 846. (b) Wang, X.; Liu, L.; Jacobson, A. J. *Angew. Chem., Int. Ed.* **2006**, *45*, 6499. (c) Alaerts, L.; Maes, M.; Giebler, L.; Jacobs, P. A.; Martens, J. A.; Denayer, J. F. M.; Kirschhock, C. E. A.; De Vos, D. E. *J. Am. Chem. Soc.* **2008**, *130*, 14170. (d) Cychosz, K. A.; Wong-Foy, A. G.; Matzger, A. J. *J. Am. Chem. Soc.* **2008**, *130*, 6938. (e) Alaerts, L.; Kirschhock, C. E. A.; Maes, M.; van der Veen, M. A.; Finsy, V.; Depla, A.; Martens, J. A.; Baron, G. V.; Jacobs, P. A.; Denayer, J. F. M.; De Vos, D. E. *Angew. Chem., Int. Ed.* **2007**, *46*, 4293.
- (4) (a) Wang, Z.; Cohen, S. M. *J. Am. Chem. Soc.* **2007**, *129*, 12368. (b) Song, Y.-F.; Cronin, L. *Angew. Chem., Int. Ed.* **2008**, *47*, 4635. (c) Wang, Z.; Cohen, S. M. *Angew. Chem., Int. Ed.* **2008**, *47*, 4699. (d) Gadzikwa, T.; Farha, O. K.; Malliakas, C. D.; Kanatzidis, M. G.; Hupp, J. T.; Nguyen, S. T. *J. Am. Chem. Soc.* **2008**, *131*, 13613. (e) Wang, Z.; Cohen, S. M. *J. Am. Chem. Soc.* **2009**, *131*, 16675. (f) Gadzikwa, T.; Farha, O. K.; Malliakas, C. D.; Kanatzidis, M. G.; Hupp, J. T.; Nguyen, S. T. *J. Am. Chem. Soc.* **2009**, *131*, 13613. (g) Jones, S. C.; Bauer, C. A. *J. Am. Chem. Soc.* **2009**, *131*, 12516.

difficulty in the adsorption and separation of reactive functional group substituted aromatics by MOFs. As we know, the separation and isolation of functional group substituted aromatics are very important, because they are of practical value and are often used as intermediates in various industrial products such as dyestuffs, drugs, and perfumes. Thus, their pure isomers are of high value. Unfortunately, aromatic isomers, due to their very similar physical and chemical properties, are very difficult to completely separate by traditional methods such as chromatography, distillation, and crystallization.<sup>5</sup> Fortunately, rationally designed self-assembled metal–organic hosts (including discrete and polymeric molecular containers) with well-defined inner cavities have provided a new chemical phase which might open the door to completely separating these reactive aromatic isomers under mild conditions.

In addition to guest storage and separation, confined spaces within self-assembled hosts can have many other wondrous properties. It is now clear that the molecular behavior within a confined space could be distinctly different from that in solution.<sup>6</sup> For example, selective encapsulation within the inner cavity of a self-assembled molecular container can change and catalyze chemical reactions<sup>7</sup> or alter magnetic<sup>8</sup> and luminescent properties.<sup>9</sup> Such unusual chemical and physical behaviors upon encapsulation certainly result from intriguing host–guest interactions. In a parallel field, utilization of a virtually unlimited range of organic spacers with the various coordination modes of diverse metal ions has generated a sufficiently large database of metal-directed hosts from which, however, only a few applications, some mentioned above, have been deduced. In principle, the hybrid nature of the metal–organic containers with polymorphic microenvironments should facilitate more chemical and physical processes within the confined spaces. Recent research in self-assembled molecular containers reflects their application in the encapsulation and stabilization of short-lived intermediates such as reactive organic,<sup>10</sup> organometallic,<sup>11</sup> and

inorganic species.<sup>12</sup> The preparation and isolation of these fleeting species as stable forms are particularly important not only in permitting spectroscopic observation but also for understanding the chemical and biological mechanisms. To date, however, the number of reported examples of this type is quite limited.

In this contribution, we report the synthesis of the series of reactive organic group functionalized aromatic guest loaded host–guest complexes  $G_n \subset CdL_2$  ( $n = 1, 2, L = 4\text{-amino-3,5-bis(4-pyridyl-3-phenyl)-1,2,4-triazole}$ ), namely  $[CdL_2(ClO_4)_2] \cdot 2(2\text{-furaldehyde})$  (2),  $[CdL_2(ClO_4)_2] \cdot 2(3\text{-furaldehyde})$  (3),  $[CdL_2(ClO_4)_2] \cdot 2(2\text{-thiophenylaldehyde})$  (4),  $[CdL_2(ClO_4)_2] \cdot (3\text{-thiophenylaldehyde})$  (5),  $[CdL_2(ClO_4)_2] \cdot (o\text{-toluidine})$  (6),  $[CdL_2(ClO_4)_2] \cdot (m\text{-toluidine})$  (7),  $[CdL_2(ClO_4)_2] \cdot (p\text{-toluidine})$  (8), and  $[CdL_2(ClO_4)_2] \cdot 2(\text{aniline})$  (9), based on a  $CdL_2$  metal–organic host ( $[Cd(L)_2(ClO_4)_2] \cdot H_2O$ , 1) in both guest vapor and liquid phases on single crystals. In addition, the  $CdL_2$  host can protect these reactive organic groups (i.e.,  $-CHO$  and  $-NH_2$  groups) in the medium of their reaction partners. Furthermore, the  $CdL_2$  host is capable of complete separations of these reactive group functionalized aromatic isomers (i.e., 2-furaldehyde vs 3-furaldehyde, 2-thiophenylaldehyde vs 3-thiophenylaldehyde, *o*-toluidine vs *m*-toluidine vs *p*-toluidine), which are directly performed on  $CdL_2$  single crystals. More interestingly, we show herein how encapsulation can render photoinduced organic radicals of these reactive functional group substituted aromatics and stabilize them in air through a constrictive mechanism under ambient conditions.

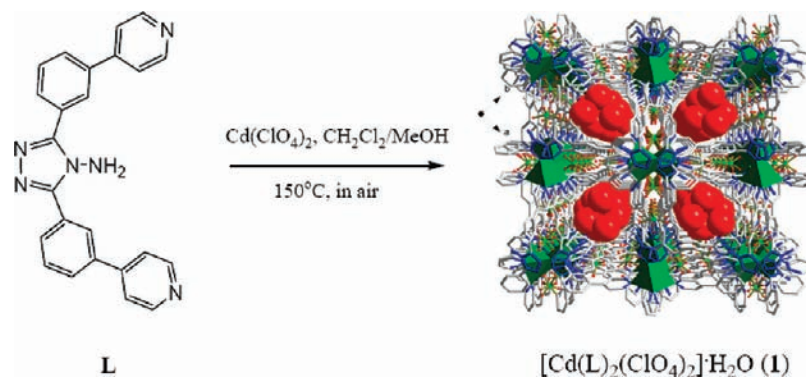
## Results and Discussion

**Synthesis and Structures of 2–9.** We have described the preparation of the three-dimensional framework of 1 ( $[Cd(L)_2(ClO_4)_2] \cdot H_2O$ ) (Scheme 1).<sup>13</sup> It contains squarelike channels with crystallographic dimensions of ca.  $11 \times 11 \text{ \AA}$ , in which the  $-NH_2$  groups on L are located at each of the squarelike cavity corners and face toward the center of the channel. The uncoordinated  $ClO_4^-$  anions are not located in the cavities but are dispersed in the framework around the channels (Scheme 1). The crystals of 1 are very stable and retain their single crystallinity until  $300 \text{ }^\circ\text{C}$ .<sup>13</sup> Thus, the guest adsorption and separation can be expediently performed on the single crystals, and the resulting host–guest complexes can be easily characterized by X-ray single-crystal analysis. It is worth noting that our previous study indicated that 1 is able to encapsulate either water or organic aromatics; therefore, the squarelike channel in 1 is amphiphilic because of the coexistence of an organic aromatic ring, an amino-substituted heterocycle, and a  $ClO_4^-$  anion. Such porous MOFs might be ideal candidates for the adsorption of polar organic guests: for example, the heteroatom-involved guest substrates.

Indeed, when the single crystals of 1 were exposed to 2-furaldehyde, 3-furaldehyde, 2-thiophenylaldehyde, 3-thiophenylaldehyde, *o*-toluidine, *m*-toluidine, *p*-toluidine, and aniline vapors, respectively ( $50 \text{ }^\circ\text{C}$ , 4 days), X-ray single-crystal structural analysis indicated that the encapsulated water molecules were readily replaced by the corresponding organic guests to generate the new host–guest systems of 2–9 (Figure 1). It is noteworthy that temperature and time parameters herein are the key factors in the formation of  $G_n \subset CdL_2$ . The higher

- (5) (a) Chow, F. K.; Grushka, E. *Anal. Chem.* **1977**, *49*, 1756. (b) Young, P. R.; McNair, H. M. *Anal. Chem.* **1975**, *47*, 756.  
 (6) Rebek, J., Jr. *Acc. Chem. Res.* **2009**, *42*, 1660.  
 (7) (a) Wang, Z.; Chen, G.; Ding, K. *Chem. Rev.* **2009**, *109*, 322. (b) Pluth, M. D.; Bergman, R. G.; Raymond, K. N. *Science* **2007**, *316*, 85. (c) Yoshizawa, M.; Tamura, M.; Fujita, M. *Science* **2006**, *312*, 251. (d) Kang, J. M.; Hilmersson, G.; Santamaria, J.; Rebek, J. *J. Am. Chem. Soc.* **1998**, *120*, 3650. (e) Hasting, C. J.; Fiedler, D.; Bergman, R. G.; Raymond, K. N. *J. Am. Chem. Soc.* **2008**, *130*, 10977. (f) Yoshizawa, M.; Takeyama, Y.; Okano, T.; Fujita, M. *J. Am. Chem. Soc.* **2003**, *125*, 3243.  
 (8) (a) Halder, G. J.; Kepert, C. J.; Moubaraki, B.; Murray, K. S.; Cashion, J. D. *Science* **2002**, *298*, 1762. (b) Ono, K.; Yoshizawa, M.; Akita, M.; Kato, T.; Tsunobuchi, Y.; Ohkoshi, S.-i.; Fujita, M. *J. Am. Chem. Soc.* **2009**, *131*, 2782. (c) Southon, P. D.; Liu, L.; Fellows, E. A.; Price, D. J.; Halder, G. J.; Chapman, K. W.; Moubaraki, B.; Murray, K. S.; Létard, J.-F.; Kepert, C. J. *J. Am. Chem. Soc.* **2009**, *131*, 10998.  
 (9) (a) Dalgarno, S. J.; Tucker, S. A.; Bassil, D. B.; Atwood, J. L. *Science* **2005**, *309*, 2037. (b) Dong, Y.-B.; Wang, P.; Ma, J.-P.; Zhao, X.-X.; Wang, H.-Y.; Tang, B.; Huang, R.-Q. *J. Am. Chem. Soc.* **2007**, *129*, 4872. (c) McManus, G. J.; Perry, J. J., IV; Perry, M.; Wagner, B. D.; Zaworotko, M. J. *J. Am. Chem. Soc.* **2007**, *129*, 9094. (d) Wang, P.; Ma, J.-P.; Dong, Y.-B.; Huang, R.-Q. *J. Am. Chem. Soc.* **2007**, *129*, 10620. (e) Wang, P.; Ma, J.-P.; Dong, Y.-B. *Chem. Eur. J.* **2009**, *15*, 10432. (f) Jiang, Y.-Y.; Ren, S.-K.; Ma, J.-P.; Liu, Q.-K.; Dong, Y.-B. *Chem. Eur. J.* **2009**, *15*, 10742.  
 (10) (a) Iwasawa, T.; Hooley, R. J.; Rebek, J., Jr. *Science* **2007**, *317*, 493. (b) Yoshizawa, M.; Kusakawa, T.; Fujita, M.; Yamaguchi, K. *J. Am. Chem. Soc.* **2000**, *122*, 6311. (c) Cram, D. J.; Tanner, M. E.; Thomas, R. *Angew. Chem., Int. Ed. Engl.* **1991**, *30*, 1024.  
 (11) (a) Leung, D. H.; Bergman, R. G.; Raymond, K. N. *J. Am. Chem. Soc.* **2007**, *129*, 2746. (b) Fielder, D.; Bergman, R. G.; Raymond, K. N. *Angew. Chem., Int. Ed.* **2006**, *45*, 745.

- (12) Mal, P.; Breiner, B.; Rissanen, K.; Nitschke, J. R. *Science* **2009**, *324*, 1697.  
 (13) Liu, Q.-K.; Ma, J.-P.; Dong, Y.-B. *Chem. Eur. J.* **2009**, *15*, 10364.

Scheme 1. Synthesis of **1**<sup>a</sup>

<sup>a</sup> The encapsulated water guests are shown in space-filling mode.

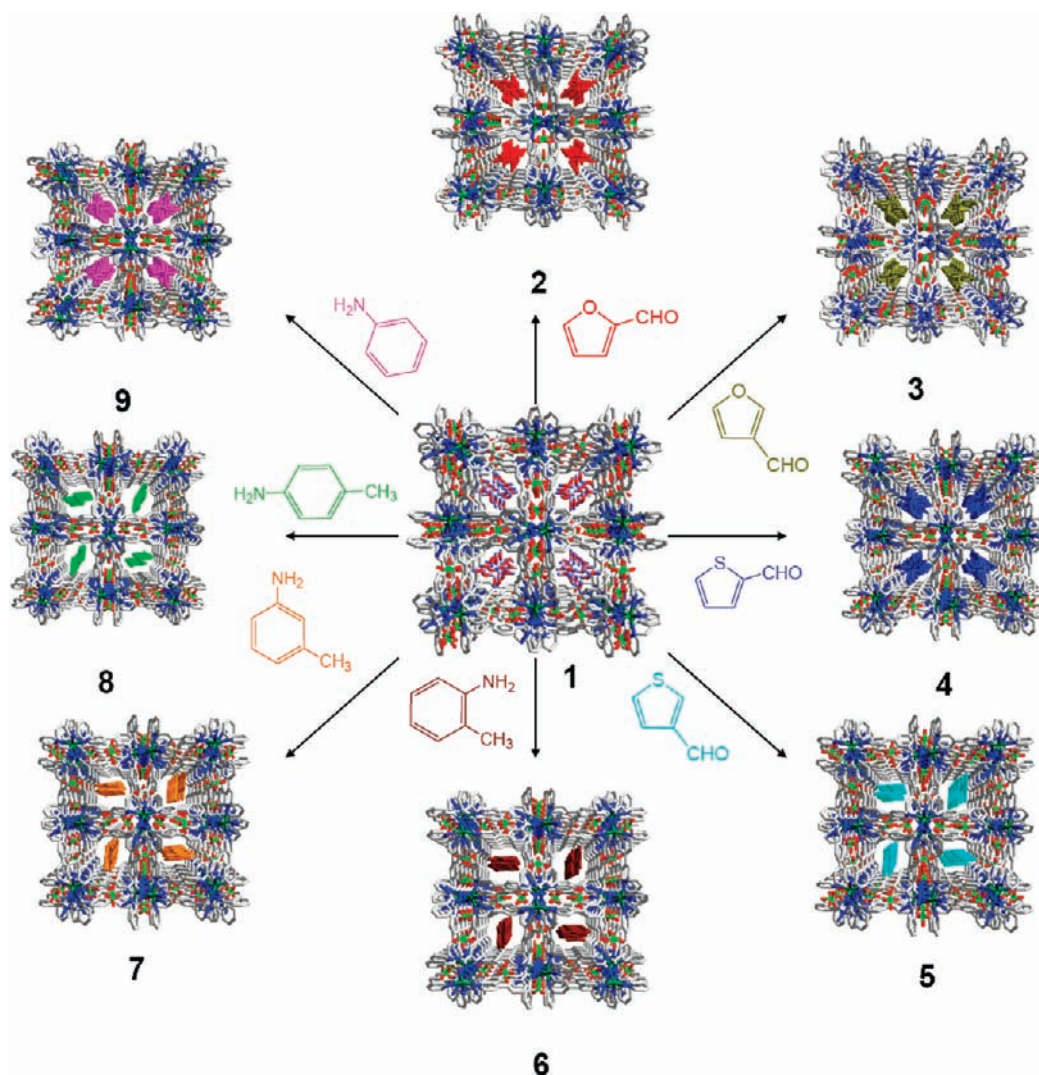


**Figure 1.** Synthesis and crystal structures of **2–9** (shown down the crystallographic *c* axis). For clarity, the different encapsulated reactive functional group substituted aromatic guests are shown in different colors.

temperature would enhance the guest exchange speed and longer exposure time would ensure that the crystals were fully saturated at lower temperature. For example, <sup>1</sup>H NMR spectra indicate that furfuraldehyde isomers and aniline can be incorporated into **1** to generate adsorption-saturated crystals of **2**, **3**, and **9** at room temperature in 1 week, while their fully saturated samples can be obtained only after 4 days at 50 °C. At room temperature,

however, only a tiny amount of thiophenylaldehyde and toluidine isomers were adsorbed by **1** in 1 week. On the other hand, the higher temperature and longer exposure time, however, would destroy the single-crystal nature of **1**. Thus, the temperature of the guest exchange in the vapor phase was eventually chosen as 50 °C. In addition, the host–guest complexes of **2–9** can also be obtained by directly immersing the single crystals of **1**



**Table 1.** Crystal Data Collection and Structure Refinement Details for Compounds 2–5

	2	3	4	5
empirical formula	C <sub>58</sub> H <sub>44</sub> CdCl <sub>2</sub> N <sub>12</sub> O <sub>12</sub>	C <sub>58</sub> H <sub>44</sub> CdCl <sub>2</sub> N <sub>12</sub> O <sub>12</sub>	C <sub>58</sub> H <sub>44</sub> CdCl <sub>2</sub> N <sub>12</sub> O <sub>10</sub> S <sub>2</sub>	C <sub>53</sub> H <sub>40</sub> CdCl <sub>2</sub> N <sub>12</sub> O <sub>9</sub> S
formula wt	1284.35	1284.35	1316.47	1204.33
temp (K)	123(2)	123(2)	123(2)	123(2)
cryst syst	tetragonal	tetragonal	tetragonal	tetragonal
space group	<i>P</i> 4 <sub>3</sub> 2 <sub>1</sub> 2	<i>P</i> 4 <sub>3</sub> 2 <sub>1</sub> 2	<i>P</i> 4 <sub>3</sub> 2 <sub>1</sub> 2	<i>P</i> 4 <sub>3</sub> 2 <sub>1</sub> 2
<i>a</i> (Å)	15.826(2)	15.937(2)	15.8318(13)	15.8731(10)
<i>b</i> (Å)	15.826(2)	15.937(2)	15.8318(13)	15.8731(10)
<i>c</i> (Å)	21.639(6)	21.884(7)	21.957(4)	21.776(3)
α (deg)	90	90	90	90
β (deg)	90	90	90	90
γ (deg)	90	90	90	90
<i>V</i> (Å <sup>3</sup> )	5419.8(18)	5559(2)	5503.5(11)	5486.5(8)
<i>Z</i>	4	4	4	4
ρ <sub>calcd</sub> (g/cm <sup>3</sup> )	1.574	1.535	1.589	1.458
<i>F</i> (000)	2616	2616	2680	2448
no. of data/restraints/params	5054/13/340	5188/19/345	5131/27/390	5113/27/386
GOF on <i>F</i> <sup>2</sup>	1.133	1.106	1.089	1.097
final <i>R</i> indices ( <i>I</i> > 2σ( <i>I</i> ))	<i>R</i> 1 = 0.0783 w <i>R</i> 2 = 0.2143	<i>R</i> 1 = 0.0578 w <i>R</i> 2 = 0.1607	<i>R</i> 1 = 0.0593 w <i>R</i> 2 = 0.1471	<i>R</i> 1 = 0.0632 w <i>R</i> 2 = 0.1690

**Table 2.** Crystal Data Collection and Structure Refinement Details for Compounds 6–9

	6	7	8	9
empirical formula	C <sub>55</sub> H <sub>45</sub> CdCl <sub>2</sub> N <sub>13</sub> O <sub>8</sub>	C <sub>55</sub> H <sub>45</sub> CdCl <sub>2</sub> N <sub>13</sub> O <sub>8</sub>	C <sub>55</sub> H <sub>45</sub> CdCl <sub>2</sub> N <sub>13</sub> O <sub>8</sub>	C <sub>60</sub> H <sub>50</sub> CdCl <sub>2</sub> N <sub>14</sub> O <sub>8</sub>
formula wt	1199.34	1199.34	1199.34	1278.44
temp (K)	123(2)	123(2)	123(2)	123(2)
cryst syst	tetragonal	tetragonal	tetragonal	tetragonal
space group	<i>P</i> 4 <sub>3</sub> 2 <sub>1</sub> 2	<i>P</i> 4 <sub>3</sub> 2 <sub>1</sub> 2	<i>P</i> 4 <sub>3</sub> 2 <sub>1</sub> 2	<i>P</i> 4 <sub>3</sub> 2 <sub>1</sub> 2
<i>a</i> (Å)	15.8496(16)	15.8832(12)	15.8800(13)	15.8508(9)
<i>b</i> (Å)	15.8496(16)	15.8832(12)	15.8800(13)	15.8508(9)
<i>c</i> (Å)	15.8496(16)	21.700(3)	21.505(3)	21.766(2)
α (deg)	90	90	90	90
β (deg)	90	90	90	90
γ (deg)	90	90	90	90
<i>V</i> (Å <sup>3</sup> )	5453.5(13)	5474.4(10)	5423.1(11)	5468.7(7)
<i>Z</i>	4	4	4	4
ρ <sub>calcd</sub> (g/cm <sup>3</sup> )	1.461	1.455	1.469	1.553
<i>F</i> (000)	2448	2448	2448	2616
no. of data/restraints/params	4812/50/392	5105/49/392	5060/17/347	5082/1/347
GOF on <i>F</i> <sup>2</sup>	1.082	1.067	1.041	1.107
final <i>R</i> indices ( <i>I</i> > 2σ( <i>I</i> ))	<i>R</i> 1 = 0.0501 w <i>R</i> 2 = 0.1294	<i>R</i> 1 = 0.0531 w <i>R</i> 2 = 0.1429	<i>R</i> 1 = 0.0521 w <i>R</i> 2 = 0.1310	<i>R</i> 1 = 0.0543 w <i>R</i> 2 = 0.1540

in 2-furaldehyde (25 °C, 6 days), 3-furaldehyde (25 °C, 8 days), 2-thiophenylaldehyde (35 °C, 10 days), 3-thiophenylaldehyde (35 °C, 12 days), *o*-toluidine (35 °C, 8 days), *m*-toluidine (35 °C, 10 days), *p*-toluidine (35 °C, 10 days), and aniline (25 °C, 6 days) liquids, respectively (Figure 1). Again, the temperatures were chosen to be as low as possible to ensure the guest exchange within a reasonable period of time in a single-crystal-to-single-crystal manner.

The relatively high quality and resolution of the diffraction data allow for unambiguous assignment of the framework conformation and the arrangement of the guest molecules within the cavities (Figure 1), although the guests are disordered to some extent, a result of high space-group symmetry. Along with the single-crystal analysis, guest incorporation into the CdL<sub>2</sub> host was further evidenced by the <sup>1</sup>H NMR spectra (Supporting Information). The thermogravimetric analysis (TGA) indicates that the encapsulated guests can be removed in the temperature range of 30–280 °C (Supporting Information).

The single-crystal structural analysis indicates that the framework of **1** does not show significant guest-independent cell volume variation (Tables 1 and 2). The different guest species in **1–9** only resulted in a 2.5% cell variation (from 5419.8(18) to 5559(2) Å<sup>3</sup>), which means that the CdL<sub>2</sub> framework is rigid. In other words, the presence of the different

aromatic guests within the channels does not have a profound effect on the architecture of framework **1**. Upon close inspection of the structures, we found that the encapsulated guests are stabilized in the channel through a guest(D–H)⋯ClO<sub>4</sub><sup>−</sup>(A)⋯host(D–H) hydrogen bonding system. As shown in Figure 2, the hydrogen bonds consist of the active functional group on the guest (–CHO or –NH<sub>2</sub>), the triazole –NH<sub>2</sub> group on the framework, and the uncoordinated ClO<sub>4</sub><sup>−</sup> anion.

**Active Functional Group Protection.** One of the important applications of metal–organic molecular containers is to protect active species. The narrow confines of a host cavity could make the encapsulated active species inert toward their reaction partners in exterior surroundings. For example, the interior confined space of molecular containers might avoid the encapsulated substrates to contact with their surrounding reaction partners<sup>14</sup> or prohibit the formation of the corresponding products which are too large for the host inner space.<sup>12</sup> It is well-known that the combination of aromatic amine with aldehyde is readily to generate imines under very mild condi-

(14) Fiedler, D.; Bergman, R. G.; Raymond, K. N. *Angew. Chem., Int. Ed.* **2006**, *45*, 745.

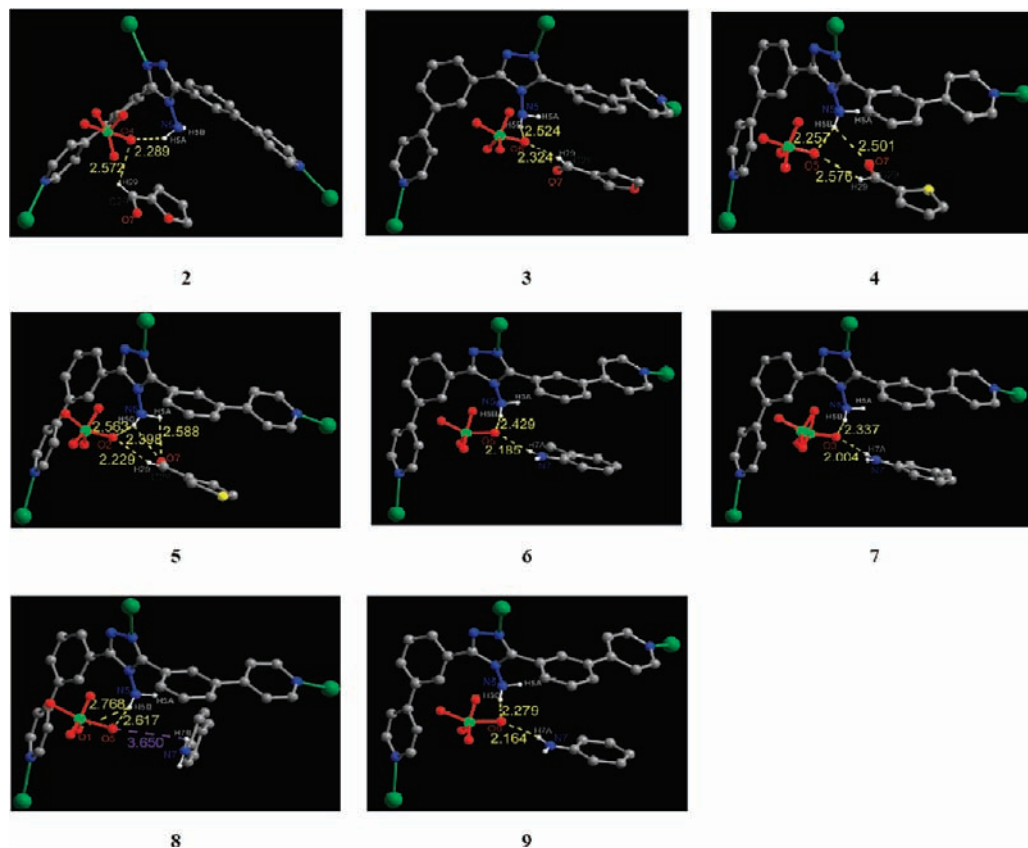


**Figure 2.** Inter-host–guest hydrogen-bonding systems in **2–9**. No strong inter-host–guest hydrogen-bonding interactions are found in **8**.

tions.<sup>15</sup> For exploration of the active organic group protecting function of CdL<sub>2</sub>, the single crystals of the heterocyclic aldehydesCdL<sub>2</sub>, that is, 2-furaldehydeCdL<sub>2</sub> (**2**), 3-furaldehydeCdL<sub>2</sub> (**3**), 2-thiophenaldehydeCdL<sub>2</sub> (**4**), and 3-thiophenaldehydeCdL<sub>2</sub> (**5**), were immersed in aniline for 24 h at room temperature; the single-crystal nature of **2–5** was still maintained. The single-crystal analysis (**2'–5'**, Supporting Information) indicated that the encapsulated guest heterocyclic aldehydes are intact. On the other hand, when *o*-toluidineCdL<sub>2</sub> (**6**), *m*-toluidineCdL<sub>2</sub> (**7**), *p*-toluidineCdL<sub>2</sub> (**8**), and anilineCdL<sub>2</sub> (**9**) were allowed to stand in formaldehyde solution for 24 h at room temperature, the single-crystal nature of **6–9** remained; again the single-crystal structure (**6'–9'**, Supporting Information) revealed that the interior aromatic amines are intact.

**Isomer Separation.** Interestingly, **1** is capable of discerning and completely separating these –CHO and –NH<sub>2</sub> functionalized aromatic isomers in both vapor and liquid phases (i. e., 2-furaldehyde vs 3-furaldehyde, 2-thiophenaldehyde vs 3-thiophenaldehyde, and *o*-toluidine vs *m*-toluidine vs *p*-toluidine) under mild conditions while retaining single crystallinity (Scheme 2).

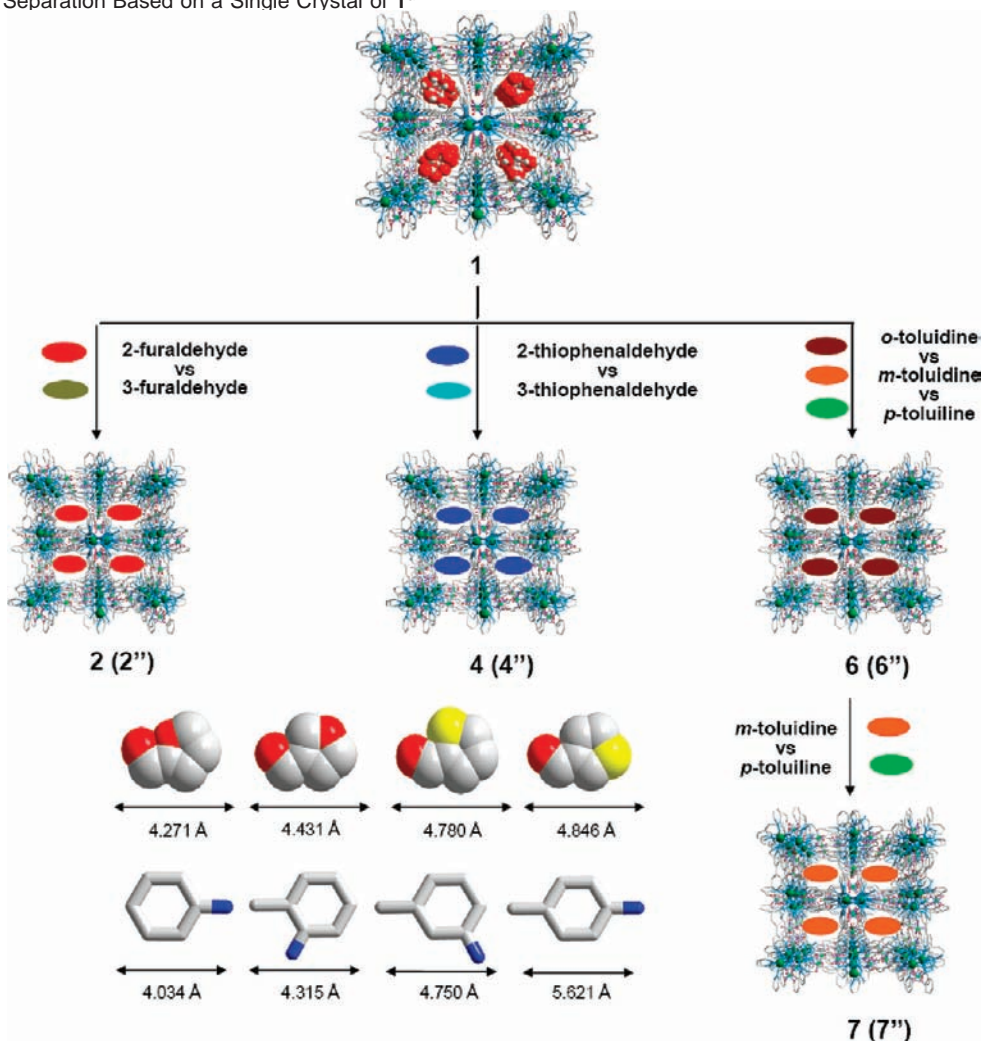
When the single crystals of **1** were exposed to a mixed vapor of equimolar amounts of 2-furaldehyde and 3-furaldehyde for 4 days at 50 °C, the single-crystal nature was still maintained. The X-ray single-crystal analysis indicated that the encapsulated water molecules were only replaced by 2-furaldehyde to give rise to **2** (**2''**; Supporting Information); meanwhile, no 3-fural-

dehyde guests were found in the channels. Such exclusive encapsulation was further confirmed by the <sup>1</sup>H NMR spectra (Figure 3). For example, as indicated in Figure 3b, no proton resonance ( $\delta$  9.90 ppm) related to the –CHO group attached to 3-furaldehyde is observed in **2''**, with respect to the exclusive adsorption of 2-furaldehyde. In addition to vapor-phase separation, **1** is still able to completely separate 2- and 3-furaldehyde in the liquid phase at room temperature. When the crystals of **1** were immersed in a mixed solvent of 2-furaldehyde and 3-furaldehyde (molar ratio, 1:1) at room temperature for 8 days, the <sup>1</sup>H NMR spectrum clearly evidenced that only the 2-furaldehyde isomer was taken up by **1** (Figure 3c).

Similarly, when the single crystals of **1** were exposed to a mixed vapor of equimolar 2- and 3-thiophenaldehyde at 50 °C for 4 days, only 2-thiophenaldehyde guests were found in the host cavities to generate **4**, which is also proved by the single-crystal analysis (**4''**, Supporting Information) and the <sup>1</sup>H NMR spectra (Figure 4). **1** again is capable of completely separating 2- and 3-thiophenaldehyde in solution. The <sup>1</sup>H NMR spectrum performed on the sample which was obtained from a solution consisting of equal amounts of 2-thiophenaldehyde and 3-thiophenaldehyde (35 °C, 12 days) clearly demonstrates that 2-thiophenaldehyde is the preferred guest for **1** over its 3-substituted isomer. The adsorption temperature chosen is based on the synthesis of compounds **4** and **5**. Hence, the 2-isomer of thiophenaldehyde can be separated from the 3-isomer in both the vapor and liquid phases.

Notably, in comparison to their 3-substituted isomers (bp: 3-furaldehyde, 145 °C; 3-thiophenaldehyde, 194 °C), 2-substituted isomers (bp: 2-furaldehyde, 162 °C; 2-thiophenaldehyde, 197 °C) have lower vapor pressures. As shown above, however,

(15) The yellow precipitate formed immediately after the combination of furaldehyde or thiophenaldehyde with aniline under ambient conditions. IR and <sup>1</sup>H NMR indicated the formation of the corresponding imines.

Scheme 2. Isomer Separation Based on a Single Crystal of **1**<sup>a</sup>

<sup>a</sup> The guest isomers are shown as ellipsoids in different colors for clarity. The crystallographic lengths of these guest molecules, which are defined as the longest distances between the non-hydrogen atoms on these guest molecules, are shown.

only 2-substituted heteroatomcyclic isomers with lower vapor pressure were preferentially encapsulated in the vapor phase without any observable amount of 3-substituted isomers. Such a result demonstrates the guest dimension is the dominating factor instead of their vapor pressures for this rigorous selectivity. Because the widths of 2-substituted isomers are almost identical with those of 3-substituted isomers, the guest lengths (4.271 and 4.431 Å for 2- and 3-furaldehyde and 4.780 and 4.846 Å for 2- and 3-thiophenylaldehyde, respectively; Scheme 2) might be a deciding factor for this selective sorption. In addition to guest size, the different functional group orientation could also play an important role in this extreme selectivity. As we know, functional group orientation is related to the guest polarity and shape. As mentioned above, the  $-\text{NH}_2$  substituted triazole moiety of the ligand and the  $\text{ClO}_4^-$  anions create a specific polar interior that might differentiate guest molecules on the basis of different polarity and shape. Thus, the affinity and strict selectivity of the isomer guest binding in **1** result from the synergy among the size, polarity, and shape of the guest substrates.<sup>16</sup>

For the case of toluidine isomers, **1** also displays strict selectivity (Scheme 2). For example, when the single crystals

of **1** were exposed to a mixed vapor of equimolar *o*-toluidine, *m*-toluidine, and *p*-toluidine for 4 days at 50 °C, only *o*-toluidine was allowed into the pores of **1** to result in **6**. Furthermore, when the single crystals of **1** were exposed to a mixed vapor of equimolar *m*-toluidine and *p*-toluidine under the same conditions, only *m*-toluidine guest was taken inside. Therefore, among the three isomers, *o*-toluidine is the preferred guest for **1** over either *m*-toluidine or *p*-toluidine. Between *m*- and *p*-toluidine, *m*-toluidine is preferred under the experimental conditions. The results are well supported by both single-crystal analysis (**6''** and **7''**; see the Supporting Information) and <sup>1</sup>H NMR spectra (Figure 5). Owing to their very similar vapor pressures (bp: 200, 203, and 200 °C for *o*-, *m*-, and *p*-toluidine, respectively), the rigorous selectivity of **1** toward toluidine isomers is again a result of the guest dimension, polarity, and shape instead of its vapor pressure. As shown herein, the smaller and more highly polar toluidine isomers are preferentially adsorbed: that is, *o*-toluidine > *m*-toluidine > *p*-toluidine.

To probe the dimension factor in this interesting selectivity further, an experiment was designed to test the binding affinity for aniline vs these three toluidine isomers (*o*-toluidine, *m*-toluidine, and *p*-toluidine). As a result, only the smallest aniline guest was incorporated into **1** to generate  $[\text{CdL}_2(\text{ClO}_4)_2] \cdot 2(\text{aniline})$  (**9**) when the crystals of **1** were exposed to a mixed

(16) Dewal, M. B.; Lufaso, M. W.; Hughes, A. D.; Samuel, S. A.; Pellechia, P.; Shimizu, L. S. *Chem. Mater.* **2006**, *18*, 4855.

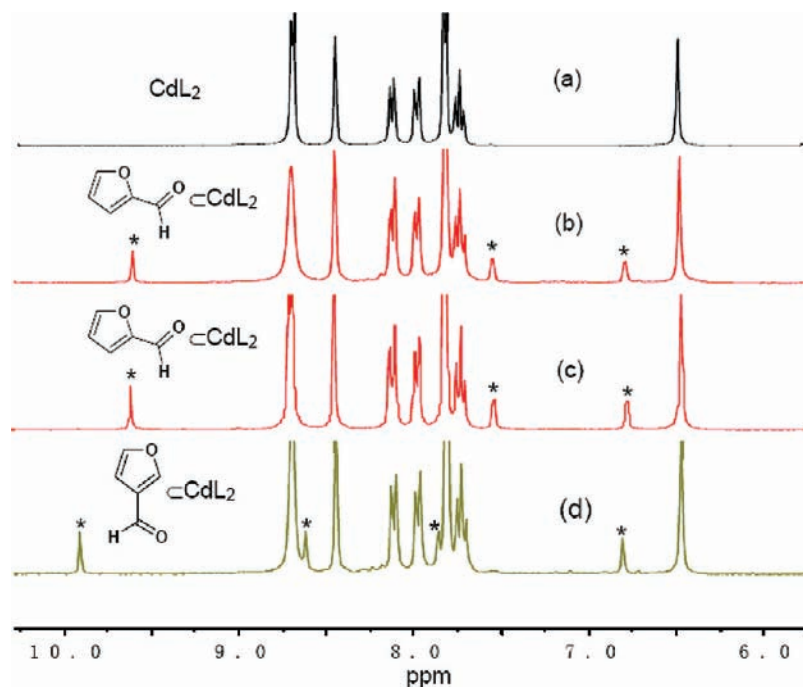


**Figure 3.** <sup>1</sup>H NMR spectra (300 MHz, DMSO-*d*<sub>6</sub>, 25 °C) of (a) **1**, (b) **1** exposed to a mixed vapor of 2- and 3-furaldehyde for ca. 4 days at 50 °C, (c) **1** immersed in a mixed liquid of 2- and 3-furaldehyde for 8 days at 25 °C, and (d) **3**. The signals marked by an asterisk correspond to the encapsulated 2-furaldehyde ( $\delta$  9.60, 8.20, 7.53, and 6.78 ppm; the peak at ca. 8.20 ppm is overlapped by the ligand signals) and 3-furaldehyde ( $\delta$  9.90, 8.862, 7.86, and 6.80 ppm), respectively.

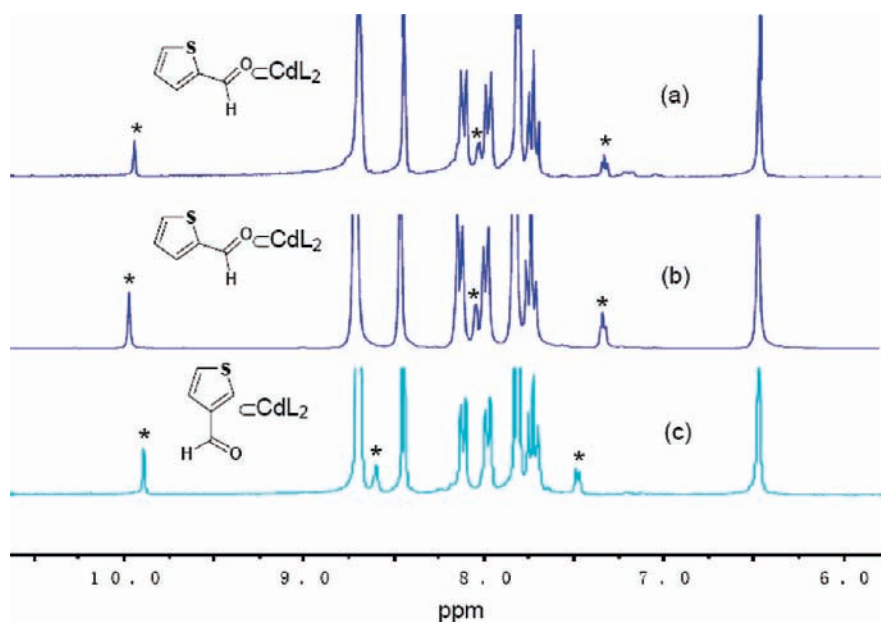


**Figure 4.** <sup>1</sup>H NMR spectra (300 MHz, DMSO-*d*<sub>6</sub>, 25 °C) of (a) **1** exposed to a mixed vapor of 2- and 3-thiophenylaldehyde for 4 days at 50 °C, (b) **1** immersed in a mixed liquid of 2- and 3-thiophenylaldehyde for 12 days at 35 °C, and (c) **5**. The signals marked by an asterisk correspond to the encapsulated 2-thiophenylaldehyde ( $\delta$  9.94, 8.15, 8.04, and 7.33 ppm; the peak at 8.04 ppm is overlapped by the ligand signals) and 3-thiophenylaldehyde ( $\delta$  9.89, 8.60, and 7.48–7.46 ppm), respectively.

vapor of these four kinds of guests at 50 °C for 4 days. Again, the result was identified by a single-crystal analysis (**9'**; Supporting Information) and <sup>1</sup>H NMR spectrum (Figure 6). For the case of aniline vs toluidine isomers, **1** clearly displays binding selectivity by dimension exclusion (aniline is  $\sim 0.3$  Å shorter than *o*-toluidine; Scheme 2), which is further confirmed by the guest adsorption amount. Single-crystal analysis unambiguously indicates that two aniline guest molecules per Cd atom are loaded in **9**. As shown above, however, only one toluidine

isomer per Cd atom can be enclathrated by **1**. Thus, we can rationalize the selectivity of **1** for the guests with the same polar functional group briefly on the basis of the guest dimension.

To explore the possibility of separating these aromatic amines in the liquid phase, the mother crystals were immersed in a mixed-solvent system that consists of equimolar aniline and *o*-, *m*-, and *p*-toluidine at 35 °C for 10 days. Similarly, aniline is the preferred guest for **1** compared to *o*-, *m*-, and *p*-toluidine. Among the *o*-, *m*-, and *p*-toluidine isomers, **1** exhibits an affinity



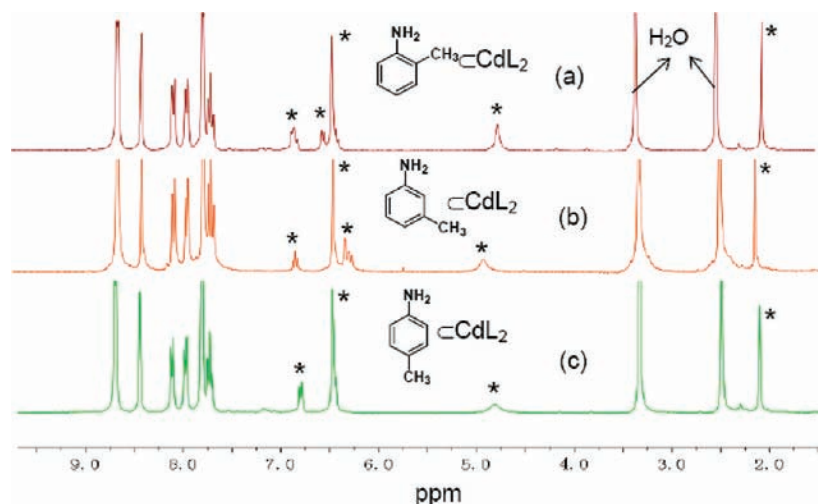


**Figure 5.**  $^1\text{H}$  NMR spectra (300 MHz,  $\text{DMSO-}d_6$ , 25  $^\circ\text{C}$ ) of (a) **1** exposed to a mixed vapor of equimolar *o*-, *m*-, and *p*-toluidine for 4 days at 50  $^\circ\text{C}$ , (b) **1** exposed to a mixed vapor of equimolar *m*- and *p*-toluidine for 4 days at 50  $^\circ\text{C}$ , and (c) **8**. The signals marked by an asterisk correspond to the encapsulated *o*-toluidine (**6**:  $\delta$  6.87–6.83, 6.58–6.55, 6.42–6.40, 4.75, and 2.02 ppm), *m*-toluidine protons (**7**:  $\delta$  6.89–6.84, 6.35–6.28, 4.92, and 2.12 ppm), and *p*-toluidine protons (**8**:  $\delta$  6.80, 6.48–6.440, 4.81, and 2.10 ppm), respectively.

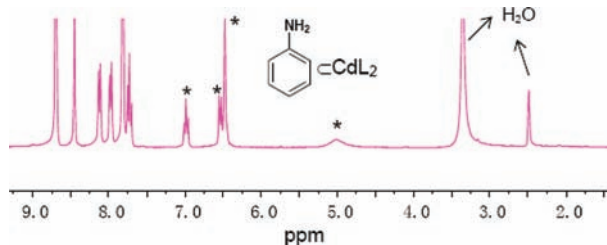


**Figure 6.**  $^1\text{H}$  NMR spectrum (300 MHz,  $\text{DMSO-}d_6$ , 25  $^\circ\text{C}$ ) of **1** isolated from a mixed vapor of equimolar aniline and *o*-, *m*-, and *p*-toluidine at 50  $^\circ\text{C}$  after 4 days. The signals marked by an asterisk correspond to the encapsulated aniline ( $\delta$  7.00–6.96, 6.55–6.52, 5.01 ppm).

for these competitors based on a sequence of *o*-, *m*-, and *p*-toluidine. The corresponding  $^1\text{H}$  NMR spectra are shown in Figure 7.

To confirm this rigorous selectivity further, a series of parallel experiments were carried out. When the crystals of **2''**, **4''**, **6''**, **7''**, and **9''** were suspended in  $\text{CD}_3\text{CN}$  at room temperature for 12 h, respectively,  $^1\text{H}$  NMR spectra on the  $\text{CD}_3\text{CN}$  extract indicate that the corresponding encapsulated guest molecules could be readily removed by solid–liquid extractions.<sup>17</sup> Upon removal of the guest molecules, the XRPD patterns (Supporting Information) of the resulting crystalline samples unambiguously demonstrated that the frameworks were maintained upon extraction, which clearly benefits from the robust nature of the framework. **1** is insoluble in  $\text{CD}_3\text{CN}$ ; therefore, the possibility of a dissolution–recrystallization mechanism for the solid–liquid extraction is certainly impossible. The  $^1\text{H}$  NMR spectra measured for the  $\text{CD}_3\text{CN}$  extracts are in good agreement with the above discussion (Supporting Information): that is, only proton resonances corresponding to the 2-furaldehyde (**2''**), 2-thiophenylaldehyde (**4''**), *o*-toluidine (**6''**), *m*-toluidine (**7''**), and aniline (**9''**) were observed, respectively.

As we know, the major hurdle in molecular separation is selectivity: that is, the preparation of the host framework that responds to only one kind of specific substrate in the presence

of one or several different potential competitors. Selective inclusion of positional isomers of inert alkylaromatics based on metal–organic frameworks has been reported recently. The *complete separation* of the inert alkylaromatics, however, has not been realized on reported MOFs. The positional isomers are always coadsorbed when the host framework is dipped into an isomer mixture.<sup>13,18</sup> To the best of our knowledge, the complete separation of positional aromatic isomers in both the vapor and liquid phase on the metal–organic framework is unprecedented, although the complete separation of organic geometrical isomers based on a Mn(II) MOF single crystal was reported very recently.<sup>19</sup>

As mentioned above, **1** displays a very strict selectivity for these reactive group substituted aromatic isomers and can completely separate them under mild conditions in both the vapor and liquid phase. The result herein thus serves as a counterpoint and important complement to the inert aromatics adsorption and separation by MOFs, which is a currently very active research area.

**Photoinduced Organic Radicals Generation and Stabilization within a Confined Space of  $\text{CdL}_2$ .** The stabilization of active species within the confined space is one of the very attractive functional properties provided by molecular containers. The finding of the existence of active guest radicals within the  $\text{CdL}_2$  framework herein is enlightened by their luminescent study. As shown in Figure 8, **1** exhibits strong emission at ca. 450 nm upon excitation at 315 nm, corresponding to a distinct blue color. After uptake of these reactive functional group substituted aromatics, the photoinduced emission spectra indicate that the emission of **1** was strongly quenched, in some cases completely, an outcome that was quite unexpected. Importantly, the closed shell ion  $\text{Cd(II)}$  was chosen for this study because it should not significantly quench the luminescence emission.<sup>20</sup> In addition, the first-generated, almost colorless crystals became darker upon

(17) (a) Hou, G.-G.; Ma, J.-P.; Sun, T.; Dong, Y.-B.; Huang, R.-Q. *Chem. Eur. J.* **2009**, *15*, 2261. (b) Jiang, Y.-Y.; Ren, S.-K.; Ma, J.-P.; Liu, Q.-K.; Dong, Y.-B. *Chem. Eur. J.* **2009**, *15*, 10742.

(18) Alaerts, L.; Kirschhock, C. E. A.; Maes, M.; van der Veen, M. A.; Finsy, V.; Depla, A.; Martens, J. A.; Baron, G. V.; Jacobs, P. A.; Denayer, J. F. M.; De Vos, D. E. *Angew. Chem., Int. Ed.* **2007**, *46*, 4293.

(19) Das, M. C.; Bharadwaj, P. K. *J. Am. Chem. Soc.* **2009**, *131*, 10942.  
(20) McManus, G. J.; Perry, J. J., IV; Perry, M.; Wagner, B. D.; Zaworotko, M. J. *J. Am. Chem. Soc.* **2007**, *129*, 9094.



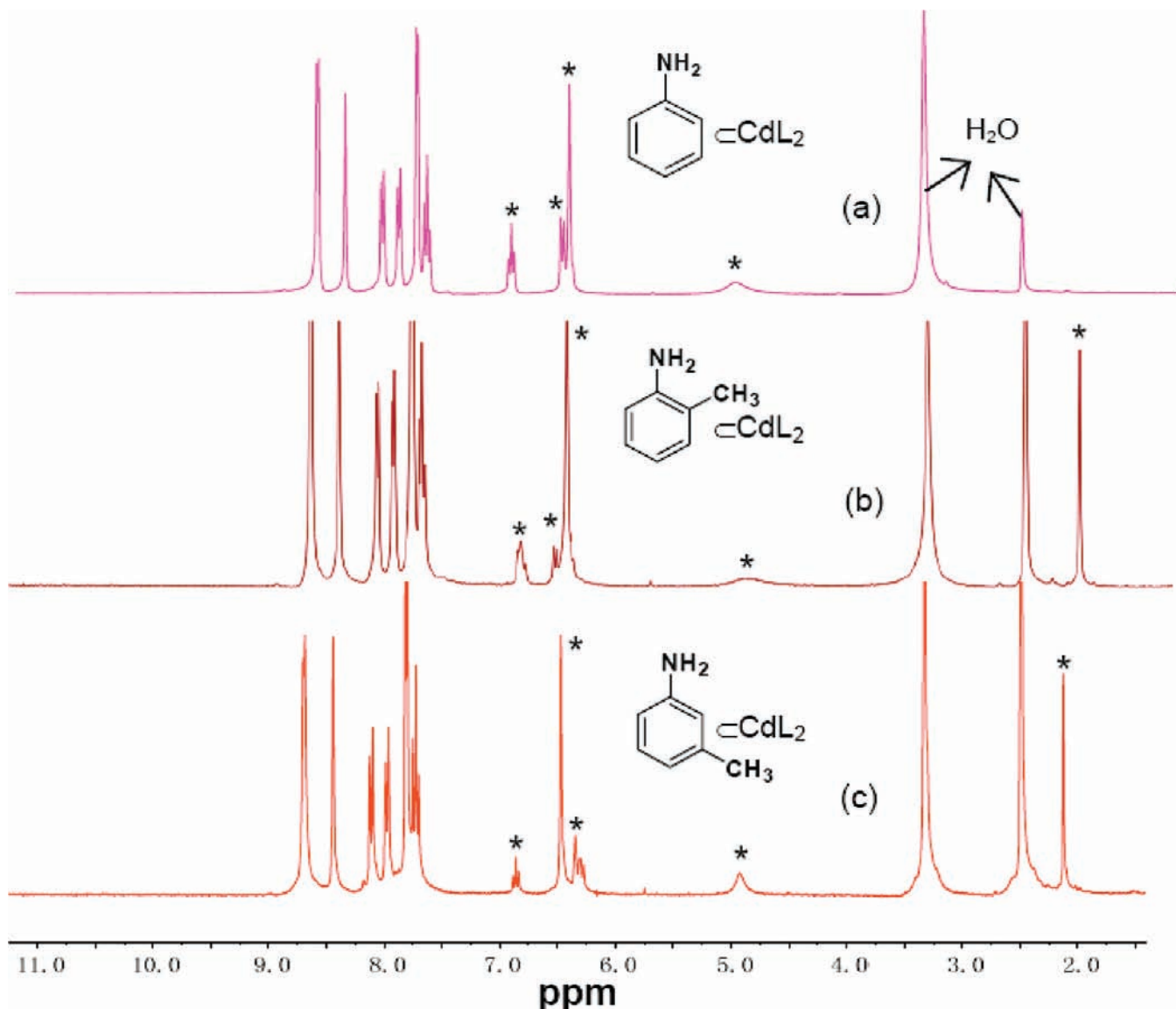


**Figure 7.**  $^1\text{H}$  NMR spectra (300 MHz,  $\text{DMSO-}d_6$ , 25  $^\circ\text{C}$ ) of (a) **1** isolated from a mixed liquid of equimolar aniline and *o*-, *m*-, and *p*-toluidine at 35  $^\circ\text{C}$  after 10 days, (b) **1** isolated from a mixed liquid of equimolar *o*-, *m*-, and *p*-toluidine at 35  $^\circ\text{C}$  after 10 days, and (c) **1** isolated from a mixed liquid of equimolar *m*- and *p*-toluidine at 35  $^\circ\text{C}$  after 10 days. The signals marked by an asterisk correspond to the encapsulated guest molecules.

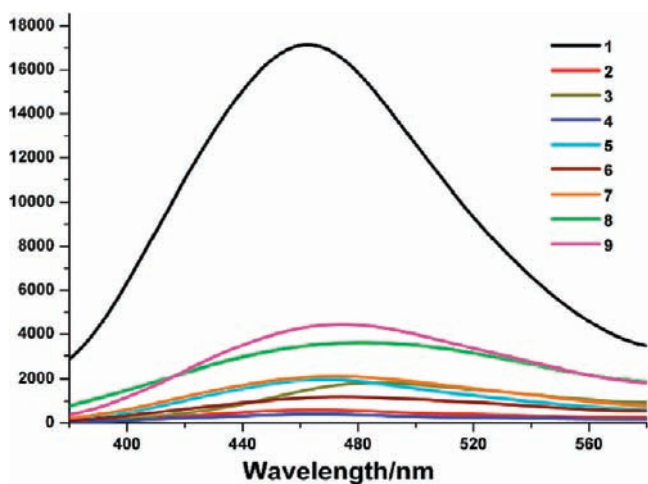


**Figure 8.** Photoinduced solid-state emission spectra of **1–9** ( $\lambda_{\text{ex}} = 315$  nm) under ambient conditions.

exposure to ambient light or UV light (Figure 9). Recently, we have demonstrated that tunable luminescence can be realized on the metal-directed host–guest systems by a guest-driven approach. Both emission color and intensity can be tuned by consciously controlling the encapsulated guest species.<sup>9b–d,21</sup> For example, the entry of inert aromatic hydrocarbons such as benzene, toluene, and *o*-, *m*-, and *p*-xylene into the  $\text{CdL}_2$  host leads to an ordered increase of the emission intensity as the guest size increases, which is logically attributed to the structural rigidity enhancement imposed by the guest inclusion.<sup>13</sup> As shown in Figure 8, the solid-state luminescent properties of  $\text{G}_n\text{CdL}_2$  (**2–9**) herein are distinctly different from those of inert aromatic hydrocarbon containing supramolecular complexes.<sup>13</sup> What did happen inside? Is it possible that unpaired electron species are generated in these host–guest systems?

(21) Wang, H.-Y.; Cheng, J.-Y.; Ma, J.-P.; Dong, Y.-B.; Huang, R.-Q. *Inorg. Chem.* **2010**, *49*, 2416.

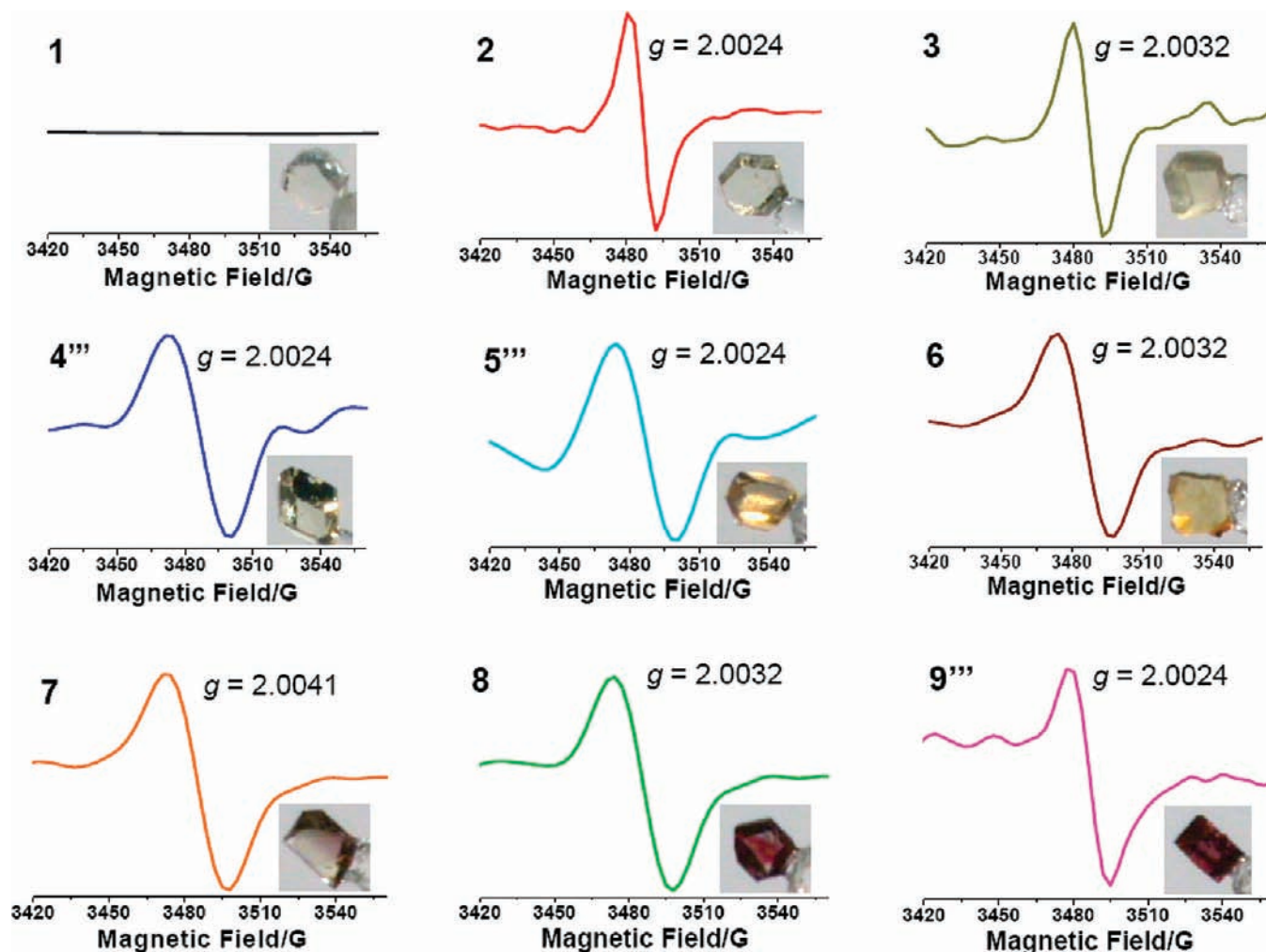


**Figure 9.** Solid-state steady-state ESR spectra of **1–9**. For **1**, no ESR signal was detected upon both ambient light and UV light irradiation (355 nm). For **2**, **3**, and **6–8**, the ESR signals were directly detected in ambient light. For **4**, **5**, and **9**, no ESR signals were detected in ambient light but the signals appeared upon UV light irradiation (355 nm). Pictures of the crystals upon exposure to ambient light or UV light are shown as inserts.

To test our hypothesis, steady-state electron spin resonance (ESR) measurements were performed on **1–9** in the solid state under ambient conditions (25 °C, ambient light and in air). As shown in Figure 9, the ESR spectrum of **1** shows no signal, while the ESR spectra of **2**, **3**, and **6–8** show a broad signal in ambient light, unequivocally demonstrating the formation of radical species. Interestingly, for **4**, **5**, and **9**, no ESR signals were detected in ambient light, but their ESR signals appeared upon 355 nm UV light irradiation (**4'''**, **5'''**, and **9'''**). **1** shows no signal even upon UV light irradiation (355 nm). All the obtained  $g$  values are in the range of 2.0024–2.0041, which confirms the formation of corresponding organic radicals.<sup>22</sup> No ESR signals from **2–9** were detected in the dark under aerobic conditions, indicating a photoinduced radical generation process instead of an oxidation process. Thus, the luminescence quenching of **1** is clearly caused by the formation of radical species. Surprisingly, once formed, these guest radicals generated from **2–9** are stable and can persist for 1 month within the host in air under ambient conditions.<sup>23</sup> Such behavior is remarkably different from the free organic radicals and the organic radicals within a previously reported host cage. Recently, Fujita et al. reported an interesting photooxidation of the alkane guest within

a Pd<sub>6</sub>L<sub>4</sub> host cage.<sup>24</sup> Therein the encapsulated photoinduced guest radical was detected in argon, and the generated radical was immediately trapped by O<sub>2</sub> or H<sub>2</sub>O from media to give the corresponding oxidized products. In the present study, however, the encapsulated radicals cannot be trapped by O<sub>2</sub> or H<sub>2</sub>O in air, probably due to the steric boundary posed by the confining framework. The reaction of O<sub>2</sub> or H<sub>2</sub>O with encapsulated radicals would produce oxidized products too large for the channel of **1**.<sup>12</sup> Such a hypothesis is supported by the fact that **1** cannot encapsulate aromatics or substituted aromatics longer than *p*-toluidine (i.e., ca. 5.7 Å), even after prolonged exposure under the experimental conditions.

As mentioned above, the encapsulated guests are stabilized in the channel through a guest(D–H)⋯ClO<sub>4</sub><sup>−</sup>(A)⋯host(D–H) hydrogen-bonding system. It is likely that the host–guest hydrogen-bonding interactions in **2–9** are critical in the

(22) Chatgililoglu, C.; Crich, D.; Komatsu, M.; Ryu, I. *Chem. Rev.* **1999**, *99*, 1993.

(23) The ESR spectra of **1–9** were measured 1 month later after their synthesis. The ESR measurement was taken in ambient light first; compounds **2**, **3**, and **6–8** displayed ESR signals but **4**, **5**, and **9** did not. After UV (355 nm) irradiation, **4**, **5**, and **9**, however, clearly displayed ESR signals. After an additional 1 month, **4**, **5**, and **9** still displayed their ESR peaks without UV light irradiation.

(24) Yoshizawa, M.; Miyagi, S.; Kawano, M.; Ishiguro, K.; Fujita, M. *J. Am. Chem. Soc.* **2004**, *126*, 9172.

**Table 3.** Crystal Data Collection and Structure Refinement Details for Compounds 2'–5'

	2'	3'	4'	5'
empirical formula	C <sub>58</sub> H <sub>44</sub> CdCl <sub>2</sub> N <sub>12</sub> O <sub>12</sub>	C <sub>58</sub> H <sub>44</sub> CdCl <sub>2</sub> N <sub>12</sub> O <sub>12</sub>	C <sub>58</sub> H <sub>44</sub> CdCl <sub>2</sub> N <sub>12</sub> O <sub>10</sub> S <sub>2</sub>	C <sub>53</sub> H <sub>40</sub> CdCl <sub>2</sub> N <sub>12</sub> O <sub>9</sub> S
formula wt	1284.35	1284.35	1316.47	1204.33
temp (K)	123(2)	123(2)	123(2)	123(2)
cryst syst	tetragonal	tetragonal	tetragonal	tetragonal
space group	<i>P</i> 4 <sub>1</sub> 2 <sub>1</sub> 2	<i>P</i> 4 <sub>3</sub> 2 <sub>1</sub> 2	<i>P</i> 4 <sub>1</sub> 2 <sub>1</sub> 2	<i>P</i> 4 <sub>3</sub> 2 <sub>1</sub> 2
<i>a</i> (Å)	15.8539(10)	15.8926(19)	15.8440(10)	15.8770(12)
<i>b</i> (Å)	15.8539(10)	15.8926(19)	15.8440(10)	15.8770(12)
<i>c</i> (Å)	21.660(3)	21.972(5)	21.837(3)	21.806(3)
α (deg)	90	90	90	90
β (deg)	90	90	90	90
γ (deg)	90	90	90	90
<i>V</i> (Å <sup>3</sup> )	5444.1(9)	5549.6(16)	5481.7(9)	5497.0(10)
<i>Z</i>	4	4	4	4
ρ <sub>calcd</sub> (g/cm <sup>3</sup> )	1.567	1.537	1.595	1.455
<i>F</i> (000)	2616	2616	2680	2448
no. of data/restraints/params	5072/16/351	5179/19/345	5110/27/390	5122/27/386
GOF on <i>F</i> <sup>2</sup>	1.110	1.052	1.078	1.165
final <i>R</i> indices ( <i>I</i> > 2σ( <i>I</i> ))	<i>R</i> 1 = 0.0638 w <i>R</i> 2 = 0.1725	<i>R</i> 1 = 0.0554 w <i>R</i> 2 = 0.1533	<i>R</i> 1 = 0.0584 w <i>R</i> 2 = 0.1425	<i>R</i> 1 = 0.0706 w <i>R</i> 2 = 0.1819

**Table 4.** Crystal Data Collection and Structure Refinement Details for Compounds 6'–9'

	6'	7'	8'	9'
empirical formula	C <sub>55</sub> H <sub>45</sub> CdCl <sub>2</sub> N <sub>13</sub> O <sub>8</sub>	C <sub>55</sub> H <sub>45</sub> CdCl <sub>2</sub> N <sub>13</sub> O <sub>8</sub>	C <sub>55</sub> H <sub>45</sub> CdCl <sub>2</sub> N <sub>13</sub> O <sub>8</sub>	C <sub>60</sub> H <sub>50</sub> CdCl <sub>2</sub> N <sub>14</sub> O <sub>8</sub>
formula wt	1199.34	1199.34	1199.34	1278.44
temp (K)	123(2)	123(2)	123(2)	123(2)
cryst syst	tetragonal	tetragonal	tetragonal	tetragonal
space group	<i>P</i> 4 <sub>1</sub> 2 <sub>1</sub> 2	<i>P</i> 4 <sub>1</sub> 2 <sub>1</sub> 2	<i>P</i> 4 <sub>3</sub> 2 <sub>1</sub> 2	<i>P</i> 4 <sub>3</sub> 2 <sub>1</sub> 2
<i>a</i> (Å)	15.8633(16)	15.8725(12)	15.8809(12)	15.8548(10)
<i>b</i> (Å)	15.8633(16)	15.8725(12)	15.8809(12)	15.8548(10)
<i>c</i> (Å)	21.760(3)	21.673(3)	21.810(3)	21.746(3)
α (deg)	90	90	90	90
β (deg)	90	90	90	90
γ (deg)	90	90	90	90
<i>V</i> (Å <sup>3</sup> )	5475.7(11)	5460.1(10)	5500.6(10)	5466.4(8)
<i>Z</i>	4	4	4	4
ρ <sub>calcd</sub> (g/cm <sup>3</sup> )	1.455	1.459	1.448	1.553
<i>F</i> (000)	2448	2448	2448	2616
no. of data/restraints/params	5102/55/392	5083/1/352	5132/17/366	5083/1/351
GOF on <i>F</i> <sup>2</sup>	1.091	1.078	1.067	1.086
final <i>R</i> indices ( <i>I</i> > 2σ( <i>I</i> ))	<i>R</i> 1 = 0.0489 w <i>R</i> 2 = 0.1329	<i>R</i> 1 = 0.0528 w <i>R</i> 2 = 0.1492	<i>R</i> 1 = 0.0563 w <i>R</i> 2 = 0.1521	<i>R</i> 1 = 0.0482 w <i>R</i> 2 = 0.1381

**Table 5.** Crystal Data Collection and Structure Refinement Details for Compounds 2'', 4'', 6'', 7'', and 9''

	2''	4''	6''	7''	9''
empirical formula	C <sub>58</sub> H <sub>44</sub> CdCl <sub>2</sub> N <sub>12</sub> O <sub>12</sub>	C <sub>53</sub> H <sub>40</sub> CdCl <sub>2</sub> N <sub>12</sub> O <sub>9</sub> S	C <sub>55</sub> H <sub>45</sub> CdCl <sub>2</sub> N <sub>13</sub> O <sub>8</sub>	C <sub>55</sub> H <sub>45</sub> CdCl <sub>2</sub> N <sub>13</sub> O <sub>8</sub>	C <sub>60</sub> H <sub>50</sub> CdCl <sub>2</sub> N <sub>14</sub> O <sub>8</sub>
formula wt	1284.35	1204.33	1199.34	1199.34	1278.44
temp (K)	123(2)	123(2)	123(2)	123(2)	123(2)
cryst syst	tetragonal	tetragonal	tetragonal	tetragonal	tetragonal
space group	<i>P</i> 4 <sub>1</sub> 2 <sub>1</sub> 2	<i>P</i> 4 <sub>1</sub> 2 <sub>1</sub> 2	<i>P</i> 4 <sub>1</sub> 2 <sub>1</sub> 2	<i>P</i> 4 <sub>1</sub> 2 <sub>1</sub> 2	<i>P</i> 4 <sub>3</sub> 2 <sub>1</sub> 2
<i>a</i> (Å)	15.8773(12)	15.8792(11)	15.8635(8)	15.8878(11)	15.8029(19)
<i>b</i> (Å)	15.8773(12)	15.8792(11)	15.8635(8)	15.8878(11)	15.8029(19)
<i>c</i> (Å)	21.684(3)	21.594(3)	21.463(2)	21.703(3)	21.845(5)
α (deg)	90	90	90	90	90
β (deg)	90	90	90	90	90
γ (deg)	90	90	90	90	90
<i>V</i> (Å <sup>3</sup> )	5466.3(10)	5444.9(9)	5401.1(7)	5478.4(9)	5455.4(15)
<i>Z</i>	4	4	4	4	4
ρ <sub>calcd</sub> (g/cm <sup>3</sup> )	1.561	1.469	1.475	1.454	1.557
<i>F</i> (000)	2616	2448	2448	2448	2616
no. of data/restraints/params	5093/15/351	5076/17/347	2912/50/392	4832/1/352	4846/1/347
GOF on <i>F</i> <sup>2</sup>	1.091	1.110	1.065	1.080	1.081
final <i>R</i> indices ( <i>I</i> > 2σ( <i>I</i> ))	<i>R</i> 1 = 0.0622 w <i>R</i> 2 = 0.1704	<i>R</i> 1 = 0.0693 w <i>R</i> 2 = 0.1682	<i>R</i> 1 = 0.0423 w <i>R</i> 2 = 0.1138	<i>R</i> 1 = 0.0544 w <i>R</i> 2 = 0.1463	<i>R</i> 1 = 0.0498 w <i>R</i> 2 = 0.1353



**Table 6.** Crystal Data Collection and Structure Refinement Details for Compounds **4'''**, **5'''**, and **9'''**

	<b>4'''</b>	<b>5'''</b>	<b>9'''</b>
empirical formula	C <sub>58</sub> H <sub>44</sub> CdCl <sub>2</sub> N <sub>12</sub> O <sub>10</sub> S <sub>2</sub>	C <sub>53</sub> H <sub>40</sub> CdCl <sub>2</sub> N <sub>12</sub> O <sub>9</sub> S	C <sub>60</sub> H <sub>50</sub> CdCl <sub>2</sub> N <sub>14</sub> O <sub>8</sub>
formula wt	1316.47	1204.33	1278.44
temp (K)	123(2)	123(2)	123(2)
cryst syst	tetragonal	tetragonal	tetragonal
space group	<i>P</i> 4 <sub>3</sub> 2 <sub>1</sub> 2	<i>P</i> 4 <sub>3</sub> 2 <sub>1</sub> 2	<i>P</i> 4 <sub>3</sub> 2 <sub>1</sub> 2
<i>a</i> (Å)	15.8271(9)	15.8721(9)	15.8562(13)
<i>b</i> (Å)	15.8271(9)	15.8721(9)	15.8562(13)
<i>c</i> (Å)	21.856(2)	21.636(3)	21.765(4)
α (deg)	90	90	90
β (deg)	90	90	90
γ (deg)	90	90	90
<i>V</i> (Å <sup>3</sup> )	5474.9(7)	5450.5(8)	5472.1(11)
<i>Z</i>	4	4	4
ρ <sub>calcd</sub> (g/cm <sup>3</sup> )	1.597	1.468	1.552
<i>F</i> (000)	2680	2448	2616
no. of data/restraints/params	5106/27/390	5079/19/351	5091/1/347
GOF on <i>F</i> <sup>2</sup>	1.077	1.140	1.080
final <i>R</i> indices ( <i>I</i> > 2σ( <i>I</i> ))	<i>R</i> 1 = 0.0521 w <i>R</i> 2 = 0.1344	<i>R</i> 1 = 0.0595 w <i>R</i> 2 = 0.1659	<i>R</i> 1 = 0.0505 w <i>R</i> 2 = 0.1416

photoinduced radical formation and stabilization.<sup>25</sup> The X-ray single-crystal analysis indicated that the guest···ClO<sub>4</sub><sup>-</sup>···host bond distances in **4**, **5**, and **9** (**4** vs **4'''**, **5** vs **5'''**, and **9** vs **9'''**) changed to some extent after UV irradiation.<sup>26</sup> Hydrogen-bonding interactions between a conjugated proton donor (D–H) and proton acceptor (A) are capable of forming a short-lived nonfluorescent or weakly fluorescent exciplex (D<sup>+</sup>–H···A<sup>-</sup>) during the course of the luminescence quenching process after photoexcitation, which is a possible luminescence quenching mechanism in solution predicted by Mataga many years ago.<sup>27</sup> However, no direct evidence for the photoinduced formation of radical species is available in his studies, because charge transfer (CT) state to ground state crossing in solution is considerably faster than radical formation. The formation of stable organic radicals within a confined space herein demonstrates that the constrictive encapsulation might facilitate the proton-coupled electron transfer assisted by the host–guest hydrogen-bonding interactions. Furthermore, it can “freeze” the generated radicals through host–guest interactions in the solid state. Further study on the organic radical formation based on CdL<sub>2</sub> is in progress.

Radicals, especially simple organic radicals, are highly reactive short-lived species, generally formed thermally or photolytically by homolytic bond cleavage or by heteroatom oxidation. They play an important role in many chemical and biological processes.<sup>28</sup> In contrast to a handful of resonance-stabilized and metal-involved stable radicals,<sup>29</sup> the isolation and stabilization of simple organic radicals under ambient conditions is generally impossible. Fortunately, self-assembled metal–organic hosts with well-defined inner cavities have provided a new

chemical phase which may open the door to isolation and stabilization of such species under ambient conditions. The CdL<sub>2</sub> host herein could be considered as a radical generator and storage vessel. More generally, it might provide applications in the generation, protection, and conservation of transient species under ambient conditions.

## Conclusion

In summary, eight new host–guest supramolecular complexes **G<sub>n</sub>CdL<sub>2</sub>** (*n* = 1, 2) have been synthesized by guest exchange in both vapor and liquid guest media. Herein, the encapsulated guest molecules in **2–9** are 2-furaldehyde, 3-furaldehyde, 2-thenaldehyde, 3-thenaldehyde, *o*-toluidine, *m*-toluidine, *p*-toluidine, and aniline, which contain reactive organic functional groups. In addition, the CdL<sub>2</sub> framework is able to protect the active functional group of –CHO or –NH<sub>2</sub> in its reaction partner. Moreover, CdL<sub>2</sub> displays a strict selectivity for these positional aromatic isomers on the basis of dimension, polarity, and shape and can completely separate them under mild conditions. More importantly, within a CdL<sub>2</sub> confined space, these reactive group substituted aromatics readily transform to the corresponding radicals upon ambient light or UV light (355 nm) irradiation. The adsorption, separation, and photoinduced radical generation experiments are directly performed on the single crystals of **1**, and all of these phenomena could be observed in single-crystal-to-single-crystal fashion. Furthermore, the generated organic radicals are alive for 1 month within the interior cavity in air under ambient conditions. Simple organic radicals are highly reactive short-lived species, and they cannot be isolated and conserved under ambient conditions. Therefore, the CdL<sub>2</sub> host herein could be considered as a radical generator and storage vessel.

## Experimental Section

**Materials and Methods.** Infrared spectroscopy (IR) samples were prepared as KBr pellets, and spectra were obtained in the

(25) Nakanishi, T.; Ohkubo, K.; Kojima, T.; Fukuzumi, S. *J. Am. Chem. Soc.* **2009**, *131*, 577.

(26) After UV light irradiation, the hydrogen bonds in **4**, **5**, and **9** changed to some extent. For **4**, the C<sub>5</sub>H<sub>3</sub>S/CHO(29)···O(5)ClO<sub>3</sub><sup>-</sup> distance contracts by 0.05 Å, while the triazole/H<sub>2</sub>N(5)···O(5)ClO<sub>3</sub><sup>-</sup> distance expands by 0.223 Å. For **5**, the C<sub>5</sub>H<sub>3</sub>S/CHO(7)···O(2)ClO<sub>3</sub><sup>-</sup> distance contracts by 0.212 Å, while the triazole/H<sub>2</sub>N(5)···O(2)ClO<sub>3</sub><sup>-</sup> distance expands by 0.025 Å. For **9**, the phenyl/H<sub>2</sub>N(7)···O(6)ClO<sub>3</sub><sup>-</sup> distance contracts by 0.073 Å and the triazole/H<sub>2</sub>N(5)···O(6)ClO<sub>3</sub><sup>-</sup> distance expands by 0.028 Å.

(27) (a) Miyasaka, H.; Tabata, A.; Kamada, K.; Mataga, N. *J. Am. Chem. Soc.* **1993**, *115*, 7335. (b) Ikeda, N.; Miyasaka, H.; Okada, T.; Mataga, N. *J. Am. Chem. Soc.* **1983**, *105*, 5206.

(28) (a) Stubbe, J.; Van der Donk, W. A. *Chem. Rev.* **1998**, *98*, 805. (b) Esker, J. L.; Newcomb, M. *Adv. Heterocycl. Chem.* **1993**, *58*, 1.

(29) (a) Büttner, T.; Geier, J.; Frison, G.; Harmer, J.; Calle, C.; Schweiger, A.; Schönberg, H.; Grützmacher, H. *Science* **2005**, *307*, 235. (b) Koide, T.; Kashiwazaki, G.; Suzuki, M.; Furukawa, K.; Yoon, M.-C.; Cho, S.; Kim, D.; Osuka, A. *Angew. Chem., Int. Ed.* **2008**, *47*, 9661. (c) Förster, C.; Klinkhammer, K. W.; Tumanskii, B.; Krüger, H.-J.; Kelm, H. *Angew. Chem., Int. Ed.* **2007**, *46*, 1156. (d) Scheer, M.; Kuntz, C.; Stubenhofer, M.; Linseis, M.; Winter, R. F.; Sierka, M. *Angew. Chem., Int. Ed.* **2009**, *48*, 2600.

4000–400  $\text{cm}^{-1}$  range using a Perkin-Elmer 1600 FTIR spectrometer.  $^1\text{H}$  NMR data were collected using a AM-300 spectrometer. Chemical shifts are reported in  $\delta$  relative to TMS. Element analyses were performed on a Perkin-Elmer Model 240C analyzer. Fluorescence measurements were carried out on a Cary Eclipse spectrofluorimeter (Varian, Australia) equipped with a xenon lamp and quartz carrier at room temperature. ESR spectra were measured with a Bruker ESR300 spectrometer using quartz sample tubes.

**Synthesis of 2–9.** Single crystals of **1** in a small open vial were sealed in a larger vial containing the corresponding guest solvent. When the single crystals of **1** were exposed to 2-furaldehyde, 3-furaldehyde, 2-thiophenylaldehyde, 3-thiophenylaldehyde, *o*-toluidine, *m*-toluidine, *p*-toluidine, and aniline vapors for around 4 days at 50  $^\circ\text{C}$ , respectively, the encapsulated water molecules were completely replaced by the corresponding guest molecules to generate the new host–guest complexes  $[\text{Cd}(\text{L})_2(\text{ClO}_4)_2] \cdot 2(2\text{-furaldehyde})(\mathbf{2})$ ,  $[\text{Cd}(\text{L})_2(\text{ClO}_4)_2] \cdot 2(3\text{-furaldehyde})(\mathbf{3})$ ,  $[\text{Cd}(\text{L})_2(\text{ClO}_4)_2] \cdot 2(2\text{-thiophenylaldehyde})(\mathbf{4})$ ,  $[\text{Cd}(\text{L})_2(\text{ClO}_4)_2] \cdot (3\text{-thiophenylaldehyde})(\mathbf{5})$ ,  $[\text{Cd}(\text{L})_2(\text{ClO}_4)_2] \cdot (o\text{-toluidine})(\mathbf{6})$ ,  $[\text{Cd}(\text{L})_2(\text{ClO}_4)_2] \cdot (m\text{-toluidine})(\mathbf{7})$ ,  $[\text{Cd}(\text{L})_2(\text{ClO}_4)_2] \cdot (p\text{-toluidine})(\mathbf{8})$ , and  $[\text{Cd}(\text{L})_2(\text{ClO}_4)_2] \cdot 2(\text{aniline})(\mathbf{9})$ . In addition, **2–9** can also be obtained by immersing the crystals of **1** in the corresponding guest solvent (2-furaldehyde (25  $^\circ\text{C}$ , 6 days), 3-furaldehyde (25  $^\circ\text{C}$ , 8 days), 2-thiophenylaldehyde (35  $^\circ\text{C}$ , 10 days), 3-thiophenylaldehyde (35  $^\circ\text{C}$ , 12 days), *o*-toluidine (35  $^\circ\text{C}$ , 8 days), *m*-toluidine (35  $^\circ\text{C}$ , 10 days), *p*-toluidine (35  $^\circ\text{C}$ , 10 days) and aniline (25  $^\circ\text{C}$ , 6 days). In the liquid phase, single crystals of **2–9** are still maintained, which was confirmed by X-ray single-crystal diffraction. The crystal data obtained are the same as those of **2–9** isolated from the vapor phase. Their  $^1\text{H}$  NMR spectra confirmed that the loaded guest species are the same as those of **2–9** isolated from the vapor phase.

**Compound 2.** IR (KBr pellet,  $\text{cm}^{-1}$ ): 3353 (ms), 3097 (w), 2850 (w), 1688 (ms), 1606 (s), 1486 (ms), 1405 (ms), 1091 (s), 1013 (ms), 798 (s), 691 (ms), 622 (s).  $^1\text{H}$  NMR (300 MHz, DMSO- $d_6$ , 25  $^\circ\text{C}$ , TMS, ppm): 9.60 (s, 1H,  $-\text{C}_5\text{H}_4\text{O}_2$ ), 8.20 (d, 1H,  $-\text{C}_5\text{H}_4\text{O}_2$ ), 7.53 (m, 1H,  $-\text{C}_5\text{H}_4\text{O}_2$ ), 6.78 (m, 1H,  $-\text{C}_5\text{H}_4\text{O}_2$ ). Anal. Calcd for  $\text{C}_{58}\text{H}_{44}\text{CdCl}_2\text{N}_{12}\text{O}_{12}$ : C, 54.24; H, 3.45; N, 13.09. Found: C, 54.19; H, 3.22; N, 12.89.

**Compound 3.** IR (KBr pellet,  $\text{cm}^{-1}$ ): 3353 (ms), 3097 (w), 2842 (w), 1683 (ms), 1606 (s), 1486 (ms), 1405 (ms), 1094 (s), 1011 (ms), 797 (s), 691 (ms), 622 (s).  $^1\text{H}$  NMR (300 MHz, DMSO- $d_6$ , 25  $^\circ\text{C}$ , TMS, ppm): 9.90 (s, 1H,  $-\text{C}_5\text{H}_4\text{O}_2$ ), 8.62 (s, 1H,  $-\text{C}_5\text{H}_4\text{O}_2$ ), 7.86 (m, 1H,  $-\text{C}_5\text{H}_4\text{O}_2$ ), 6.80 (m, 1H,  $-\text{C}_5\text{H}_4\text{O}_2$ ). Anal. Calcd for  $\text{C}_{58}\text{H}_{44}\text{CdCl}_2\text{N}_{12}\text{O}_{12}$ : C 54.24; H, 3.45; N, 13.09. Found: C, 54.07; H, 3.21; N, 12.98.

**Compound 4.** IR (KBr pellet,  $\text{cm}^{-1}$ ): 3350 (ms), 3274 (w), 3098 (w), 2841 (w), 1672 (ms), 1606 (s), 1486 (ms), 1405 (ms), 1209 (ms), 1095 (s), 1011 (ms), 797 (s), 690 (ms), 622 (s).  $^1\text{H}$  NMR (300 MHz, DMSO- $d_6$ , 25  $^\circ\text{C}$ , TMS, ppm): 9.94 (s, 1H,  $-\text{C}_5\text{H}_4\text{OS}$ ), 8.15 (d, 1H,  $-\text{C}_5\text{H}_4\text{OS}$ ), 8.04 (d, 1H,  $-\text{C}_5\text{H}_4\text{OS}$ ), 7.33 (m, 1H,  $-\text{C}_5\text{H}_4\text{OS}$ ). Anal. Calcd for  $\text{C}_{58}\text{H}_{44}\text{CdCl}_2\text{N}_{12}\text{O}_{10}\text{S}_2$ : C, 52.92; H, 3.37; N, 12.77; Found: C, 52.88; H, 3.14; N, 12.61.

**Compound 5.** IR (KBr pellet,  $\text{cm}^{-1}$ ): 3350 (ms), 3278 (w), 3096 (w), 2821 (w), 1687 (ms), 1606 (s), 1486 (ms), 1403 (ms), 1235 (ms), 1093 (s), 1011 (ms), 795 (s), 690 (ms), 622 (s).  $^1\text{H}$  NMR (300 MHz, DMSO- $d_6$ , 25  $^\circ\text{C}$ , TMS, ppm): 9.89 (s, 1H,  $-\text{C}_5\text{H}_4\text{OS}$ ), 8.60 (s, 1H,  $-\text{C}_5\text{H}_4\text{OS}$ ), 7.48–7.46 (m, 2H,  $-\text{C}_5\text{H}_4\text{OS}$ ). Anal. Calcd for  $\text{C}_{53}\text{H}_{40}\text{CdCl}_2\text{N}_{12}\text{O}_9\text{S}$ : C, 52.86; H, 3.35; N, 13.96. Found: C, 52.63; H, 3.22; N, 13.68.

**Compound 6.** IR (KBr pellet,  $\text{cm}^{-1}$ ): 3347 (w), 3073 (w), 1605 (s), 1486 (ms), 1404 (ms), 1091 (s), 1010 (ms), 796 (s), 688 (ms), 621 (s).  $^1\text{H}$  NMR (300 MHz, DMSO- $d_6$ , 25  $^\circ\text{C}$ , TMS, ppm): 6.87–6.83 (m, 2H,  $-\text{C}_7\text{H}_9\text{N}$ ), 6.58–6.55 (d, 1H,  $-\text{C}_7\text{H}_9\text{N}$ ), 6.42–6.40 (m, 1H,  $-\text{C}_7\text{H}_9\text{N}$ ), 4.75 (s, 2H,  $-\text{C}_7\text{H}_9\text{N}$ ), 2.02 (s, 3H,  $-\text{C}_7\text{H}_9\text{N}$ ). Anal. Calcd for  $\text{C}_{55}\text{H}_{45}\text{CdCl}_2\text{N}_{13}\text{O}_8$ : C, 55.08; H, 3.78; N, 15.18. Found: C, 54.85; H, 3.55; N, 15.02.

**Compound 7.** IR (KBr pellet,  $\text{cm}^{-1}$ ): 3384 (w), 3093 (w), 1605 (s), 1486 (ms), 1403 (ms), 1091 (s), 1010 (ms), 797 (s), 689 (ms), 621 (s).  $^1\text{H}$  NMR (300 MHz, DMSO- $d_6$ , 25  $^\circ\text{C}$ , TMS, ppm): 6.89–6.84 (t, 1H,  $-\text{C}_7\text{H}_9\text{N}$ ), 6.35–6.28 (m, 3H,  $-\text{C}_7\text{H}_9\text{N}$ ), 4.92 (s, 2H,  $-\text{C}_7\text{H}_9\text{N}$ ), 2.12 (s, 3H,  $-\text{C}_7\text{H}_9\text{N}$ ). Anal. Calcd for  $\text{C}_{55}\text{H}_{45}\text{CdCl}_2\text{N}_{13}\text{O}_8$ : C, 55.08; H, 3.78; N, 15.18. Found: C, 54.74; H, 3.54; N, 15.01.

**Compound 8.** IR (KBr pellet,  $\text{cm}^{-1}$ ): 3348 (w), 3074 (w), 1605 (s), 1486 (ms), 1404 (ms), 1092 (s), 1010 (ms), 796 (s), 689 (ms), 622 (s).  $^1\text{H}$  NMR (300 MHz, DMSO- $d_6$ , 25  $^\circ\text{C}$ , TMS, ppm): 6.81–6.79 (d, 2H,  $-\text{C}_7\text{H}_9\text{N}$ ), 6.48–6.44 (m, 2H,  $-\text{C}_7\text{H}_9\text{N}$ ), 4.81 (s, 2H,  $-\text{C}_7\text{H}_9\text{N}$ ), 2.10 (s, 3H,  $-\text{C}_7\text{H}_9\text{N}$ ). Anal. Calcd for  $\text{C}_{55}\text{H}_{45}\text{CdCl}_2\text{N}_{13}\text{O}_8$ : C, 55.08; H, 3.78; N, 15.18. Found: C, 54.84; H, 3.43; N, 14.98.

**Compound 9.** IR (KBr pellet,  $\text{cm}^{-1}$ ): 3349 (w), 3071 (w), 1605 (s), 1486 (ms), 1404 (ms), 1091 (s), 1010 (ms), 797 (s), 689 (ms), 621 (s).  $^1\text{H}$  NMR (300 MHz, DMSO- $d_6$ , 25  $^\circ\text{C}$ , TMS, ppm): 7.00–6.96 (t, 2H,  $-\text{C}_6\text{H}_7\text{N}$ ), 6.55–6.52 (m, 3H,  $-\text{C}_6\text{H}_7\text{N}$ ), 5.01 (s, 2H,  $-\text{C}_6\text{H}_7\text{N}$ ). Anal. Calcd for  $\text{C}_{60}\text{H}_{50}\text{CdCl}_2\text{N}_{14}\text{O}_8$ : C, 56.37; H, 3.94; N, 15.34. Found: C, 56.15; H, 3.61; N, 15.27.

**Single-Crystal Structure Determination.** Suitable single crystals of complexes were selected and mounted in air onto thin glass fibers. X-ray intensity data were measured at 123(2) K on a Bruker SMART APEX CCD-based diffractometer (Mo  $\text{K}\alpha$  radiation,  $\lambda = 0.71073 \text{ \AA}$ ). The raw frame data for the complexes were integrated into SHELX-format reflection files and corrected for Lorentz and polarization effects using SAINT.<sup>30</sup> Corrections for incident and diffracted beam absorption effects were applied using SADABS.<sup>30</sup> None of the crystals showed evidence of crystal decay during data collection. All structures were solved by a combination of direct methods and difference Fourier syntheses and refined against  $F^2$  by full-matrix least-squares techniques. Non-hydrogen atoms were refined with anisotropic displacement parameters during the final cycles. Hydrogen atoms bonded to carbon and nitrogen were placed in geometrically idealized positions with isotropic displacement parameters set to  $1.2U_{\text{eq}}$  of the attached atom. The oxygen-bonded hydrogen atoms were placed in geometrically idealized positions with isotropic displacement parameters set to  $1.5U_{\text{eq}}$  of the attached atom. Crystal data, data collection parameters, and refinement statistics are given in Tables 1–6. Further details of the structural refinements for **2–9** are given in the Supporting Information.

**Acknowledgment.** This work was supported by the National Natural Science Foundation of China (Grant No. 20871076), the Shangdong Natural Science Foundation (Grant No. JQ200803), Ph.D. Programs Foundation of the Ministry of Education of China (Grant No. 200804450001), and 973 the Program (Grant No. 2007CB936000).

**Supporting Information Available:** CIF files for **2–9**, **2'–9'**, **2''**, **4''**, **6''**, **7''**, **9''**, **4'''**, **5'''**, and **9'''**, text giving details of the structure refinement, and figures giving  $^1\text{H}$  NMR spectra, TGA traces, and XRPD patterns. This material is available free of charge via the Internet at <http://pubs.acs.org>.

JA101807C

(30) SAINT and SADABS; Bruker Analytical X-ray Systems, Inc.: Madison, WI, 1998.